Published in final edited form as:
Cell Physiol Biochem. 2012 ; 30(3): 735–748. doi:10.1159/000341453.

Construction of Conditional Acid Ceramidase Knockout Mice and *in vivo* Effects on Oocyte Development and Fertility

Efrat Eliyahu[1,*], **Nataly Shtraizent**[1,2,*], **Ruth Shalgi**[2], and **Edward H. Schuchman**[1]

[1]Department of Genetics and Genomic Sciences, Mount Sinai School of Medicine, 1425 Madison Avenue, Room 14-20A, New York, NY

[2]Department of Developmental and Cell Biology, Sackler School of Medicine, Tel Aviv University, Tel Aviv

Abstract

The number of resting follicles in the ovary and their successful maturation during development define the fertile female lifespan. Oocytes, enclosed within follicles, are subject to natural selection, and the majority will undergo apoptosis during prenatal life through adulthood. Our previous studies revealed high levels of the lipid hydrolase, acid ceramidase (AC), in human and mouse oocytes, follicular fluid and cumulus cells. In addition, supplementation of *in vitro* fertilization media with recombinant AC enhanced the survival of oocytes and preimplantation embryos. Herein we constructed and used a conditional knockout mouse model of AC deficiency (cACKO) to further investigate the role of this enzyme in oocyte survival *in vivo*. Immunohistochemical staining, activity assays, and western blot analysis revealed that AC expression was high in the ovaries of normal mice, particularly in the theca cells. After induction of the AC gene knockout with tamoxifen (TM), AC levels decreased in ovaries, and ceramide was correspondingly elevated. A novel immunostaining method was developed to visualize follicles at various stages, and together with light microscopic examination, the transition of the follicle from the secondary to antral stage was found to be defective in the absence of AC. Western blot analysis showed elevated BAX and PARP expression in TM-treated cACKO mouse ovaries compared to control animals. In parallel, the levels of BCL-2 and anti-Mullerian hormone, a marker of ovarian reserve, were decreased. In addition to the above, there was a significant decrease in fertility observed in the TM-treated cACKO mice. Together, these data suggest that AC plays an important role in the preservation of fertility by maintaining low ceramide levels and preventing apoptosis of theca cells, thereby promoting survival of the follicle during the transition from the secondary to antral stage.

Keywords

Ceramide; Ovaries; Oocytes; Survival

Edward H. Schuchman, PhD, Department of Genetics & Genomic Sciences, Mount Sinai School of Medicine, Room 14-20A, NY, NY 10029 (USA), Tel. +1 212-659-6711, Fax +1 212-849-2447, Edward.Schuchman@mssm.edu.
* Both authors contributed equally to this work

Competing Interests

E.E., N.S., and E.H.S. are inventors on patents related to acid ceramidase. These patents describe the use of acid ceramidase for oocyte and embryo survival, and could in the future generate royalty income for Mount Sinai and the inventors.

Introduction

The sphingolipid hydrolase, acid ceramidase (AC, E.C. 3.5.1.23), plays an essential role in regulating cell fate by maintaining a critical balance between the pro-apoptotic lipid, ceramide, and the anti-apoptotic lipid, sphingosine-1-phosphate (S1P) [1]. The importance of AC during development is demonstrated by the fact that knockout of the murine AC gene (*Asah1*) leads to early embryonic death at the 4-cell stage, indicating that its activity cannot be compensated by other ceramidases [2, 3]. Moreover, mutations in the human AC gene result in the severe developmental disorder, Farber Lipogranulomatosis [4]. We have further shown by immunohistochemical, western blotting and enzymatic activity assays that AC is expressed in human and murine oocytes and/or follicular fluid, and that its expression levels decline during oocyte culture. In addition, supplementation of AC into media improved the survival rates and quality of oocytes and embryos grown *in vitro*, as well as embryo development *in vivo* after implantation [5].

Oocytes are enclosed within the functional unit of the ovary, the follicle, surrounded by somatic granulosa cells. Most follicles present at birth are in a state of growth arrest, and are referred to as primordial follicles in which the oocyte is surrounded by one flat layer of granulosa cells. Growth of the primordial follicle results in the differentiation of the flat granulosa cells to a cubical shape, and growth of multiple layers of granulosa, basement membrane and theca interna cells in the secondary follicle stage. Further development includes formation of a cavity between the granulosa cells, leading to transformation of secondary into antral follicles [6, 7]. This stage is also characterized by formation of theca externa. Theca cells are fundamental for follicular growth, providing hormonal, nutritional and structural support. Moreover, their function appears to be altered in certain causes of infertility [8].

Oocytes are subject to natural selection during development, and the majority will undergo apoptosis starting from prenatal life through menopause [9]. The female reproductive potential is therefore determined by the size of the oocyte pool at birth, as well as the rate of oocyte depletion during the female lifespan. Tilly and colleagues were the first to suggest that the sphingolipid signaling pathway plays an important role in oocyte survival [10]. These investigators used S1P *ex vivo* to prevent developmental apoptosis of oocytes and apoptotis induced by anti-cancer therapy, and also showed that mice lacking acid sphingomyelinase (an enzyme that produces ceramide) had suppressed apoptotic deletion of fetal oocytes, leading to neonatal ovarian hyperplasia [11–13].

In the present study we hypothesize that AC plays an essential role in ovarian development through the regulation of sphingolipid metabolism and apoptosis, and that decreased activity of this enzyme may lead to premature exhaustion of the ovarian reserve by elevation of ceramide and apoptosis. To investigate this hypothesis, we constructed a conditional AC knockout mouse (cACKO) to study the function of AC during ovarian folliculogenesis and its role in fertility. The results showed that reduction of AC activity in the ovary, particularly in the theca cells, leads to apoptosis at the secondary to antral follicle transition, and a significant reduction in fertility. This is the first report of a conditional AC knockout mouse, the first *in vivo* depiction of AC expression and localization in the ovary, and the first documentation of the important role of AC in folliculogenesis and fertility.

Materials and Methods

Mice

Mice were housed under standard conditions (19–22°C, 12h light/dark cycle) in cages with *ad libitum* access to water and food. All animal protocols were approved by the Mount Sinai Institutional Animal Care and Use Committee.

Generation of conditional knockout mice

A targeting construct (Fig. 1A) was created in which a neo expression cassette was inserted within intron 10 of the murine AC gene, flanked by FRT sites. LoxP sites also were inserted within introns 8 and 13 of the murine AC genomic fragment. This insertion allows deletion of the sequences from exons 9–13 following TM-mediated Cre recombinase translocation to the nucleus. ES cell electroporation of this targeting vector, G418 selection, expansion of gene-targeted ES cell clones, and blastocyst injections and re-implantation, were carried out by the InGenious Targeting Laboratory (Brookhaven, New York). Two hundred and eighty-eight G418 resistant colonies were obtained and analyzed for the presence of targeting events by PCR, genomic Southern blotting and sequencing. Of these, three clones contained appropriate targeting events by all screening methods, and one was used for injection into mouse blastocysts to obtain chimeric animals. The chimeras were backcrossed to C57Bl/6J mice to create F1 mice, and several of these offspring contained the targeted vector in their tail DNA. These were used to establish a breeding colony and to obtain mice that were homozygous for the targeting construct (i.e., “Floxed” mice).

The Floxed mice were then bred to Cre transgenic mice to generate AC knockout animals (cACKO) that were homozygous for the Floxed AC allele and heterozygous for the Cre allele. The inducible Cre mice used for this study were B6.Cg-Tg(cre/Esr1)5Amc/J (from Jackson Laboratories). These transgenic mice ubiquitously express a tamoxifen-inducible Cre driven by the chicken beta actin promoter/enhancer coupled with the cytomegalovirus (CMV) immediate-early enhancer [14]. The expressed Cre is a fusion product with the mutant form of the mouse estrogen receptor ligand-binding domain. This domain does not bind natural ligand at physiological concentrations, but will bind the synthetic ligand, 4-hydroxytamoxifen (TM). Restricted to the cytoplasm, the Cre/Esr1 protein can only gain access to the nuclear compartment after exposure to TM.

To induce the gene rearrangement in the cACKO mice, TM was administered to the mice through 5 consecutive IP injections at 5 weeks of age (2 mg/injection). Gene excision and phenotype was evaluated 4 months following the last injection.

DNA extraction and PCR genotyping

Genomic DNA was extracted from tissue biopsies using the DNeasy kit (Invitrogen), and genotyping was performed using specific oligonucleotides and Accuprime DNA polymerase (Invitrogen). Below is the list of primers used for this study.

For detection of the Floxed allele:

WT/Floxed intron 8 forward (P1):

ATG AGA AGT GGG TGT CAG GCG TGG

WT/Floxed intron 8 reverse (P2):

ACG TTC ATT TAG TGA AAG ACT GAA CAG CC

WT/Floxed intron 13 forward (P3):

TCC TAT CAA CAA AAC CTG TCC TCA ACA A

WT/Floxed intron 13 reverse (P4):

AGC CTT GAC TTT GGG GCA CAG AG

For detection of the Cre/Esr construct:

WT forward (P5): *CGA GGC CAC AGA ATT GAA AGA TCT*

WT reverse (P6): *GTA GGT GGA AAT TCT AGC ATC TC*

Cre forward (P7): *GCG GTC TGG CAG TAA AAA CTA TC*

Cre reverse (P8): *GTG AAA CAG CAT TGC TGT CAC TT*

For detection of the AC gene rearrangement:

Forward 1 (same as WT/Floxed intron 8 forward) (P1):

ATG AGA AGT GGG TGT CAG GCG TGG

Forward 2 (same as WT/Floxed intron 13 forward) (P3):

TCC TAT CAA CAA AAC CTG TCC TCA ACA A

Reverse (same as WT/Floxed intron 13 reverse) (P4):

AGC CTT GAC TTT GGG GCA CAG AG

RNA extraction and RT-PCR

RNA was extracted from ovarian biopsies using the TRIzol reagent (Invitrogen) according to the manufacturer's protocol. An equal amount of RNA was reverse transcribed using the Superscript III first strand kit (Invitrogen, cat# 18080-051). mRNA levels were analyzed by qPCR using Accuprime DNA polymerase and SYBR green fluorescent DNA-binding dye, and forward and reverse primers specific for AC and SRP18 (see sequences below). The PCR products were analyzed using an ABI PRISM 7900 HT sequence detection system (Applied Biosystems). Fluorescence signals were analyzed during each of 40 cycles (denaturation, 30s at 94°C; annealing, 30s at 55°C; and extension, 30s at 72°C).

Relative quantification was calculated using the comparative threshold cycle (C_T) method, as described in User Bulletin #2, ABI PRISM 7900HT Sequence Detection System. Median C_T of triplicate measurements was used to calculate DC_T as the difference in C_T for the target gene (AC) and reference (SRP18). ΔC_T values for each sample were compared with the corresponding mean control ΔC_T and expressed as $\Delta\Delta C_T$. Relative quantification was expressed as fold change of the gene of interest compared with the control according to the formula $2^{-\Delta\Delta C_T}$. Target gene expression between experimental and control groups were then compared using mean fold changes.

AC forward: *TAA CCG CAG AAC ACC GGC C*

AC reverse: *TTG ACC TTT GGT AAC ATC CAT C*

RPS18 forward: *TTC GGA ATC GAG GCC ATG AT*

RPS18 reverse: *TTT CGC TCT GGT CCG TCT TG*

Protein extraction

Proteins were extracted from ovarian tissues using a pellet pestle motor homogenizer and universal lysis buffer (Hepes 20mM, NaCl 150mM, 0.2mM Igepal pH 7.4). The extracts were clarified by centrifugation at 10,000g at 4°C.

AC activity assay

A fluorescently labeled substrate, NBD C12-ceramide, was purchased from Cayman Chemical (cat# 10007958), and a modified AC activity method was used [15]. Briefly, protein extracts from ovarian tissues were incubated at 37°C with 0.2mM of the NBD substrate in 0.1M citrate/phosphate buffer, pH 4.5, 150mM NaCl, 0.05% BSA, and 0.1% Igepal CA-630. The reactions were stopped by ethanol, centrifuged, and the supernatants were analyzed using a UPLC ACUITY separation system (Waters). Fluorescence was quantified using a fluorescence detector set to excitation and emission wavelengths of 435 and 525nm, for the product (i.e., NBD-conjugated C12-fatty acid) and substrate, respectively. The amount of product was calculated using a regression equation that was established from a standard curve using NBD-conjugated C12-fatty acid.

Histology

Ovaries were collected from euthanized female mice. From each animal, one ovary was subjected to genotype analysis to assess the extent of AC gene rearrangement, and another fixed in 4% paraformaldehyde in PBS. Fixed ovaries were dehydrated by sequential incubation in sucrose solutions in PBS (5%–2 hours, 10%–2 hours, 20%–overnight). Following dehydration, ovaries were pre-incubated in OCT (optimal cutting temperature compound) for 1 hour at room temperature (RT) and frozen in OCT on a dry ice-ethanol mix. Frozen blocks were kept at −20°C until evaluation. Cryopreserved ovaries were cut and sectioned using a cryostat (Leica CM1900), and every 5th (10mm) section was collected for follicle counting. Intermediate sections were used for other types of immunostaining.

Immunostaining

The frozen sections were dried at RT overnight and fixed in paraformaldehyde (4% in PBS) for 10 minutes at RT followed by incubation in chilled methanol for 10 minutes on ice. Slides were blocked for 2 hours at RT using 10% FBS in PBS and labeled with specific antibodies. Localization of the primary antibodies was visualized using a fluorescent second antibody (Cy-3-conjugated) and laser-scanning confocal microscopy (Zeiss LSM510).

The following antibodies were used for immunostaining:

Rabbit anti-PARD6a polyclonal antibody (Santa Cruz Biotechnologies, sc-14405), rabbit anti-AMH polyclonal antibody (Santa Cruz Biotechnologies, sc-6886), goat anti-AC polyclonal antibody (Santa Cruz Biotechnologies, sc-28486), and mouse anti-ceramide monoclonal antibody (Alexis Biochemicals, MID15B4).

Follicle counting

Light microscopy, combined with DNA labeling with Hoechst, was used to quantify the primary through antral follicle stages. Follicles were counted as primary if they contained an oocyte and were surrounded by a single layer of cuboidal shaped granulosa cells; as secondary (preantral) if they contained an intact oocyte, more than one layer of granulosa cells and lacked antral spaces; and as antral if they contained an intact oocyte, more than one layer of granulosa cells and antral spaces. To avoid double-counting follicles, only follicles containing an oocyte with a visible nucleus were counted (see Fig. 4 for a representative ovary section and examples of follicles at each stage).

To assist in the visualization of the follicles, a new immunostaining method also was developed. The PARD6a antibody was used to detect oocytes within early stage (primordial, primary, early secondary) follicles, and the anti-AMH antibody was used to label granulosa cells and visualize follicles in the secondary through early antral stages. The stereo investigator software (MBF Bioscience) was used to quantify the average number per

section at each stage. Quantitative analysis was performed on every 5th section. The total number of follicles/ovary was calculated by multiplying the average number per section by the number of sections obtained. To avoid bias, all ovaries were analyzed without knowledge of genotype.

Western blot analysis

Samples were separated by SDS-PAGE using 12% precast Nupage Bis/Tris gels under reducing conditions and MES running buffer (Invitrogen), and then transferred onto nitrocellulose membranes (Amersham Biosciences) using a semidry transfer apparatus (Bio-Rad) and Nupage-MOPS transfer buffer. For immunoblot analysis, membranes were blocked with TBS/Tween containing 5% dry milk, and then incubated with specific antibodies that were recognized by secondary antibodies conjugated to HRP. Detection was achieved using an enhanced chemiluminescence (ECL) detection reagent (Amersham Biosciences). Approximate molecular masses were determined by comparison with the migration of prestained protein standards (Bio-Rad).

The following antibody reagents were used for western blotting from Santa Cruz Biotechnology:

Anti-AC goat polyclonal IgG, cat# sc-28486; anti-Bax rabbit polyclonal IgG, cat# sc-526; anti-AMH rabbit polyclonal antibody, cat# sc-6886; anti-PARP rabbit polyclonal IgG, cat# sc-7150; anti-Bcl2 rabbit polyclonal antibody, cat# sc-7150; anti-Sox 9 goat polyclonal antibody, cat# 20095, and donkey anti-goat IgG-horseradish peroxidase (HRP) conjugate, cat# sc-2020. Goat anti-rabbit IgG-HRP conjugate also was purchased from GE Healthcare, cat# NA9340V.

Fertility studies

TM-treated Floxed or cACKO females at 3 months of age were used to set up mating pairs with wild type males of proven fertility. One Floxed and one cACKO female was placed in the cage with same male, and pregnancy was monitored by observation of the shape of the lower abdomen and increase in weight. Fertility rate was determined by analyzing the number of births per number of mating pairs.

Statistical analyses

All experiments were repeated at least three times. The combined data from triplicate experiments were subjected to t-test analysis and the p-values are indicated in each figure when applicable.

Results

Construction of the conditional AC knockout mice

The cACKO mice (homozygous for the Floxed AC allele and heterozygous for the inducible Cre, Fig. 1A) were generated as described in the Materials and Methods. To induce the AC knockout, TM was administered to 5-week-old cACKO females i.p. (2 mg/injection) once a day for 5 consecutive days. Assessment of the AC gene excision was performed 4 months following the last TM injection. DNA was extracted from skin (tail) and ovaries of TM-treated Floxed and cACKO animals. The TM-treated Floxed animals were included as controls since they lacked the Cre allele.

Fig. 1A shows a schematic depiction of the Floxed and cACKO alleles, and Fig. 1B shows representative genotyping results of DNA extracted from the tails and ovaries. Note that the efficiency of the AC gene excision in the skin of cACKO mice was 100% following TM

injection, while in the ovary of the same mouse the gene excision was partial: i.e., ~70% exhibited the 310 bp band consistent with the excised gene product. DNA of TM-treated Floxed animals showed exclusively the 250 bp band. The mosaic nature of the AC gene excision in the ovary of the cACKO mice can be attributed to variability in TM penetration into different layers of the ovarian tissue following i.p injection, and/or accessibility of the DNA to the Cre/Esr* recombinase at different stages of oocyte and follicular maturation.

Decreased ovarian AC expression in TM-treated cACKO mice

To further assess the effectiveness of the AC gene excision in the ovary, AC protein and mRNA levels were determined in TM-treated cACKO mice compared to TM-treated Floxed mice, wild-type and heterozygous complete AC knockout mice [3]. TM-treated cACKO mice had significantly decreased expression of the AC mRNA (Fig. 2A, p=1.7E-4 vs. Floxed + TM; p=4.02E-6 vs. wild-type; 2E-2 vs. heterozygous complete AC knockout) and protein (Fig. 2B) compared to any of the control animals. Consistent with the above results, AC activity also was significantly decreased in ovarian tissue from the TM-treated cACKO mice (Fig. 2C, 6E-3 vs. Floxed + TM; 3E-4 vs. wild-type; 1E-3 vs. heterozygous complete knockout). No significant differences were observed between the three control groups.

Decreased fertility in TM-treated cACKO mice

To assess whether AC depletion affected fertility, mating pairs were assembled following TM injection of Floxed or cACKO female mice, and the number of pregnancies and births in both groups was recorded (Table 1). Normal male mice were used for mating. While four of thirteen TM-injected cACKO mice were pregnant at day 17 (determined by weight gain and shape of the lower abdomen), the number of births was negligible, as only one cACKO female gave birth to one pup, which died shortly thereafter. In contrast, in the control group (TM-treated Floxed mice), ten of twelve females went though pregnancy and successfully delivered. Therefore, fertility, defined as the number of births per number of matings, was significantly decreased in the cACKO compared to Floxed group (7% vs. 83%, respectively).

Decreased ovarian reserve and elevated apoptosis in the ovary of TM-treated cACKO mice

A molecular marker of ovarian reserve, anti-Mullerian hormone (AMH), and its transcription factor, Sox9, were used to assess ovarian reserve (Fig. 3A). The pro-apoptotic markers, Bax and PARP, and the anti-apoptotic BCL-2, were used to assess apoptosis in the ovary (Fig. 3B). For these analyses ovarian protein extracts were prepared from TM-treated Floxed (control) and cACKO mice, and then analyzed by western blotting. Beta-actin was used as a loading control. The results showed that in the ovary of TM-treated cACKO mice, compared to Floxed mice, the levels of AMH, Sox9 and BCL-2 were decreased, while the levels of Bax and PARP were increased (Fig. 3A, B), suggesting that in the TM-treated cACKO mice the decreased ovarian reserve can be attributed to apoptotic cell death.

Decreased number of antral follicles in TM-treated cACKO ovaries

To assess the number of follicles at various stages in TM-treated Floxed and cACKO mice, ovaries were cryopreserved and frozen sections were either examined by light microscopy or by immunostaining as described in the Materials and Methods. A representative light microscopic image of the ovary showing the different follicle stages can be seen in Fig. 4. We also developed a new method using PARD6a and AMH antibody staining to assist in the visualization and quantification of the follicles. Of note, this method allowed analysis of the cryosections at high magnification, while moving through a defined grid and marking of the follicles at different stages. PARD6a is expressed in oocytes during the early stages of folliculogenesis [16], and assisted in the visualization of primary and early secondary

follicles (Fig. 5A). Anti-AMH stains granulosa cells [17, 18] and detects follicles at later stages (secondary through early antral) (Fig. 5B). The number of follicles at the primary, secondary and antral stages was recorded based on a combination of light and confocal examination of the immunostained sections.

The percent of follicles at each stage was compared between TM-treated cACKO and Floxed mice and the cumulative data is shown in Fig. 5C. TM-treated cACKO mice had significantly fewer antral follicles compared to TM-treated Floxed mice (40% decrease in the cACKO group, $p<0.0002$), consistent with the decreased fertility shown in Table 1. Differences in the number of primary and secondary follicles were not statistically significant.

Decreased AC expression in theca cells

To investigate the mechanism underlying the loss of antral follicles, immunostaining of ovaries from TM-treated cACKO and Floxed mice was performed using anti-AC and anti-ceramide antibodies (Fig. 6A–C). AC expression was most pronounced in the theca cells of WT or TM-injected Floxed mice, and was decreased in the TM-treated cACKO mice (Fig. 6A). Ceramide levels also were elevated in the connective tissue of the ovary and in theca cells of early antral follicles of TM-treated cACKO compared to Floxed mice (Fig. 6B,C). The most definitive difference was the ceramide level in the oocytes themselves, principally in the primary and secondary follicles. These results suggest that apoptosis in the TM-treated cACKO mice is initiated within the oocyte at the primary and secondary stages of folliculogenesis, followed by impaired theca cell development and manifested by apoptosis of antral follicles. The few remaining antral follicles are presumably those that escaped apoptosis induced by the AC gene excision.

Discussion

AC is a key enzyme responsible for maintaining ceramide levels in cells [19–21], and also is a major enzyme responsible for producing sphingosine and ultimately the pro-survival lipid, sphingosine 1-phosphate (S1P). AC and its role in ceramide-mediated apoptosis has been the subject of numerous recent studies (see for reviews [22, 23]), and inhibitors of this enzyme are currently being developed for cancer therapy e.g., [24, 25].

The mechanisms by which ceramide can lead to cellular or organism aging and/or cell death are diverse and involve signaling by ceramide itself, or in some cases by its breakdown product, sphingosine [26]. Ceramide has been described as a key regulator of morphological changes and checkpoints, interfering with spindle assembly and binding to DNA transcription factors [27, 28]. Ceramide production within cell membranes also leads to reorganization of signaling platforms, frequently resulting in apoptosis [1]. Together, these ceramide-related changes can lead to cell cycle arrest and/or cell death.

Apoptosis occurs naturally in the mammalian ovary during development and remains prominent throughout postnatal life [10]. Ceramide also has been shown to play a central role in the age-related acceleration of apoptosis in the female germline [10, 11]. In our previous publication [5], we showed that in human oocytes AC co-localizes with membranes, the meiotic spindle, and DNA, thus supporting its potential role in preventing cell cycle arrest. Recent reports also have shown that apoptosis in the ovaries of several species can be prevented by S1P, a downstream product of AC activity [11, 12, 29]. All of the above are in agreement with our hypothesis that AC has an important protective function during oocyte and follicle development.

The current study reports the first generation of a conditional AC knockout mice, and assessment of the effect of AC inactivation on ovarian folliculogenesis and mouse fertility. The results revealed that AC depletion leads to infertility due to apoptosis of oocytes during the transition of the follicles from the secondary to antral stages. Elevated levels of apoptosis markers (Bax and PARP) and decreased levels of an important marker of ovarian reserve, AMH, as well as anti-apoptotic BCL-2, support the above observation.

During the course of these studies we also developed a new immunostaining method to assist in the identification and quantification of follicles. PARD6a (also known as PAR6) is expressed in primordial follicles during prenatal development, and plays a role in the determination of cell polarity [16]. Its expression in the postnatal ovary has never been described, and we found that it is expressed in the oocytes of primary and early secondary follicles. The major benefit of anti-PARD6a staining is that it allowed oocyte-specific staining, versus other types of staining methods such as H & E, which stains all structures of the ovary. AMH is expressed postnatally in the granulosa cells surrounding the follicles from the early primary to antral stage [17, 18]. AMH staining in late primary through late secondary follicles overlapped with PARD6a, providing an additional level of confirmation during the follicle counting procedure. It also permitted better discrimination of small follicles from other structures of the ovary.

An interesting observation from this work is that high-level expression of AC was seen in the theca cell layer surrounding the follicles at the late primary and secondary stages of folliculogenesis. The importance of the transition from preantral to antral stages is supported by previous publications showing that this stage is the most susceptible to follicular atresia [30, 31]. Expression of AC in theca cells could be a prerequisite of oocyte survival during this transition. Follicular growth during this period is tightly regulated by oocyte-granulosatheca cell interactions [32]. Our observation of elevated levels of ceramide in the oocyte present in the primary and secondary follicle of TM-treated cACKO mice is consistent with the data of decreased ovarian reserve. As previously described, ceramide can be transferred from granulosa cells into the oocyte [13]. We also speculate that AC may be secreted from theca cells and transported into the oocyte to allow regulation of ceramide levels and oocyte survival. The secretion and reuptake properties of AC have been shown previously in other cell types [33].

Of note, it is not known whether ceramide can be produced within oocytes, or if it is derived from other supporting cells such as granulosa or theca. Moreover, how ceramide is transported between and within the various follicular cells is unknown. The recent construction of ceramide synthase knockout mice could help address these questions [34, 35]. In addition, it will be important to examine the role of ceramide transfer protein (CERT) in ceramide trafficking within the ovary, since in other cells disruption of CERT is detrimental to normal embryonic development [36, 37]. Sphingomyelin hydrolysis by sphingomyelinases also may be an important source of ceramide in the ovary, and at least one of these sphingomyelinases (acid sphingomyelinase, ASM) has been shown to have an important influence on oocyte development [11]. Indeed, it has already been suggested that the presence of ceramide in the nucleus may be attributed to this enzyme [38]. These and other key questions regarding ceramide metabolism in the ovary should be the subject of further investigations.

Clearly, the ceramide/sphingosine/S1P rheostat is critical to follicular development and oocyte survival, and based on our data we propose that AC is a major regulator of this pathway. Future investigations should further examine the mechanism underlying these findings, for example by studying the effect of granulosa factors, which stimulate the development of theca cells, on the expression of AC and its transport into oocytes.

Acknowledgments

The authors thank Patrick R. Hof and Bridget Wicinski (Department of Neuroscience, Mount Sinai) for assistance with the stereology microscopy. We would also like to thank Dr. Xingxuan He for assistance with the AC activity assays.

Funding

This work was supported in part by grants from the NIH (R01 DK54830) and US-Israel BiNational Foundation (2009212).

References

1. Grassmé H, Riethmüller J, Gulbins E. Biological aspects of ceramide-enriched membrane domains. Prog Lipid Res. 2007; 46:161–170. [PubMed: 17490747]
2. Eliyahu E, Park JH, Shtraizent N, He X, Schuchman EH. Acid ceramidase is a novel factor required for early embryo survival. FASEB J. 2007; 21:1403–1409. [PubMed: 17264167]
3. Li CM, Park JH, Simonaro CM, He X, Gordon RE, Friedman AH, Ehleiter D, Paris F, Manova K, Hepbildikler S, Fuks Z, Sandhoff K, Kolesnick R, Schuchman EH. Insertional mutagenesis of the mouse acid ceramidase gene leads to early embryonic lethality in homozygotes and progressive lipid storage disease in heterozygotes. Genomics. 2002; 79:218–224. [PubMed: 11829492]
4. Sugita M, Dulaney J, Moser HW. Ceramidase deficiency in Farber's disease (lipogranulomatosis). Science. 1975; 178:1100–1103. [PubMed: 4678225]
5. Eliyahu E, Shtraizent N, Martinuzzi K, Barritt J, He X, Wei H, Chaubal S, Copperman AB, Schuchman EH. Acid ceramidase improves the quality of cultured oocytes and embryos and the outcome of in vitro fertilization. FASEB J. 2010; 24:1229–1238. [PubMed: 20007509]
6. Sherwood, L. Human Physiology: From Cells to System. 8. Brooks/ Cole; United States: 2012. Formation of the antrum; p. 769
7. Tsafrir, A.; Dekel, N. Intra- and intercellular molecular mechanisms in the regulation of meiosis in muroid rodents. In: Tosti, E.; Bone, R., editors. Oocyte Maturation and Fertilization: A Long History for a Short Event. Bentham Science Publishers; Brussum, The Netherlands: 2010. p. 38-63.
8. Young JM, McNeilly AS. Theca: the forgotten cell of the ovarian follicle. Reprod. 2010; 140:489–504.
9. Jin X, Xiao LJ, Zhang XS, Liu YX. Apoptosis in the ovary. Front Bioscie. 2011; 3:680–697.
10. Morita Y, Tilly JL. Oocyte apoptosis: like sand through an hourglass. Dev Biol. 1999; 213:1–17. [PubMed: 10452843]
11. Morita Y, Perez GI, Paris F, Miranda S, Ehleiter D, Haimovitz-Friedman A, Fuks Z, Xie Z, Reed JC, Schuchman EH, Kolesnick RN, Tilly JL. Oocyte apoptosis is suppressed by disruption of the acid sphingomyelinase gene or by sphingosine-1-phosphate therapy. Nat Med. 2000; 6:1109–1114. [PubMed: 11017141]
12. Paris F, Perez GI, Haimovitz-Friedman A, Nguyen H, Fuks Z, Bose M, Ilagan A, Hunt PA, Morgan WF, Tilly JL, Kolesnick R. Sphingosine-1-phosphate preserves fertility in irradiated female mice without propagating genomic damage in offspring. Nat Med. 2006; 8:901–902. [PubMed: 12205432]
13. Perez GI, Jurisicova A, Matikainen T, Moriyama T, Kim MR, Takai Y, Pru JK, Kolesnick RN, Tilly JL. A central role for ceramide in the age-related acceleration of apoptosis in the female germline. FASEB J. 2005; 19:860–862. [PubMed: 15728664]
14. Bockamp E, Sprengel R, Eshkind L, Lehmann T, Braun JM, Emmrich F, Hengstler JG. Conditional transgenic mouse models: From basics to genome-wide sets of knockouts and current studies of tissue regeneration. Regen Med. 2008; 3:217–235. [PubMed: 18307405]
15. Tani M, Okino N, Mitsutake S, Ito M. Specific and sensitive assay for alkaline and neutral ceramidases involving C12-NBD-ceramide. J Biochem. 1999; 125:746–749. [PubMed: 10101288]
16. Wen J, Zhang H, Mao G, Chen X, Wand J, Guo M, Mu X, Ouyang H, Zhang M, Xia G. PAR6, a potential marker for germ cells selection to form primordial follicles in mouse ovary. Plos One. 2009; 4:e7372. [PubMed: 19809506]

17. Durlinger AL, Visser JA, Themmen AP. Regulation of ovarian function: the role of anti-Mullerian hormone. Reprod. 2002; 124:601–609.

18. Durlinger AL, Gruijters MJ, Kramer P, Karels B, Ingraham HA, Nachtigal MW, Uilenbroek JT, Grootegoed JA, Themmen AP. Anti-Müllerian hormone inhibits initiation of primordial follicle growth in the mouse ovary. Endocrin. 2002; 143:1076–1084.

19. Chen WW, Moser AB, Moser HW. Role of lysosomal acid ceramidase in the metabolism of ceramide in human skin fibroblasts. ABB. 1981; 208:444–455. [PubMed: 7259198]

20. Li CM, Hong SB, Kopal G, He X, Linke T, Hou WS, Koch J, Gatt S, Sandhoff K, Schuchman EH. Cloning and characterization of the full-length cDNA and genomic sequences encoding murine acid ceramidase. Genomics. 1998; 50:267–274. [PubMed: 9653654]

21. Linke T, Wilkening G, Sadeghlar F, Mozcall H, Bernardo K, Schuchman EH, Sandhoff K. Interfacial regulation of acid ceramidase activity. Stimulation of ceramide degradation by lysosomal lipids and sphingolipid activator proteins. J Biol Chem. 2000; 276:5760–5768. [PubMed: 11104761]

22. Mao C, Obeid LM. Ceramidases: Regulators of cellular responses mediated by ceramide, sphingosine, and sphingosine-1-phosphate. Biochim Biophys Acta. 2008; 1781:424–434. [PubMed: 18619555]

23. Park JH, Schuchman EH. Acid ceramidase and human disease. Biochim Biophys Acta. 2006; 1758:2133–2138. [PubMed: 17064658]

24. Flowers M, Fabrias G, Delgado A, Casas J, Abad JL, Cabot MC. C6-ceramide and targeted inhibition of acid ceramidase induce synergistic decreases in breast cancer cell growth. Breast Cancer Res Treat. 2012; 133:447–458. [PubMed: 21935601]

25. Zeidan YH, Jenkins RW, Korman JB, Liu X, Obeid LM, Norris JS, Hannun YA. Molecular targeting of acid ceramidase: implications to cancer therapy. Curr Drug Targets. 2008; 9:653–661. [PubMed: 18691012]

26. Woodcock J. Sphingosine and ceramide signaling in apoptosis. IUBMB Life. 2006; 58:462–466. [PubMed: 16916783]

27. Ogretmen B, Kraveka JM, Schady D, Usta J, Hannun YA, Obeid LM. Molecular mechanisms of ceramide-mediated telomerase inhibition in the A549 human lung adenocarcinoma cell line. J Biol Chem. 2001; 276:32506–32514. [PubMed: 11441001]

28. Swanton C, Marani M, Pardo O, Warne PH, Kelly G, Sahai E, Elustondo F, Chang J, Temple J, Ahmed AA, Brenton JD, Downward J, Nicke B. Regulators of mitotic arrest and ceramide metabolism are determinants of sensitivity to paclitaxel and other chemotherapeutic drugs. Cancer Cell. 2007; 11:498–512. [PubMed: 17560332]

29. Zelinski MB, Murphy MK, Lawson MS, Jurisicova A, Pau KYF, Toscano NP, Jacob DS, Fanto JK, Casper RF, Dertinger SD, Tilly JL. In vivo delivery of FTY720 prevents radiation-induced ovarian failure and infertility in adult female nonhuman primates. Fert Steril. 2011; 95:1440–1445.

30. Hirshfield AN. Development of follicles in the mammalian ovary. Int Rev Cytol. 1991; 124:43–101. [PubMed: 2001918]

31. McGee EA, Hsueh AJ. Initial and cyclic recruitment of ovarian follicles. Endocr Rev. 2000; 21:200–214. [PubMed: 10782364]

32. Orisaka M, Orisaka S, Jiang JY, Craig J, Wang Y, Kotsuji F, Tsang BK. Growth differentiation factor 9 is antiapoptotic during follicular development from preantral to early antral stage. Mol Endocrinol. 2006; 20:2456–2468. [PubMed: 16740654]

33. He X, Okino N, Dhami R, Dagan A, Gatt S, Schulze H, Sandhoff K, Schuchman EH. Purification and characterization of recombinant, human acid ceramidase. Catalytic reactions and interactions with acid sphingomyelinase. J Biol Chem. 2003; 278:32978–32985. [PubMed: 12815059]

34. Jennesmann R, Rabionet M, Gorgas K, Epstein S, Dalpke A, Rothermel U, Bayerle A, van der Hoeven F, Imgrund S, Kirsch J, Bickel W, Willecke K, Riezman H, Grone HJ, Sandhoff R. Loss of ceramide synthase 3 causes lethal skin barrier disruption. Hum Mol Genet. 2012; 21:586–608. [PubMed: 22038835]

35. Pewzner-Jung Y, Park H, Laviad EL, Silva LC, Lahiri S, Stiban J, Erez-Roman R, Brügger B, Sachsenheimer T, Wieland F, Prieto M, Merrill AH Jr, Futerman AH. A critical role for ceramide

synthase 2 in liver homeostasis: I. Alterations in lipid metabolic pathways. J Biol Chem. 2010; 285:10902–109910. [PubMed: 20110363]

36. Granero-Moltó F, Sarmah S, O'Rear L, Spagnoli A, Abrahamson D, Saus J, Hudson BG, Knapik EW. Goodpasture antigen-binding protein and its spliced variant, ceramide transfer protein, have different functions in the modulation of apoptosis during zebrafish development. J Biol Chem. 2008; 283:20495–20504. [PubMed: 18424781]
37. Hanada K, Kumagai K, Tomishige N, Yamaji T. CERT-mediated trafficking of ceramide. BBA Mol Cell Biol Lipids. 2009; 1791:684–691.
38. Farooqui AA, Ong WY, Farooqui T. Lipid mediators in the nucleus: Their potential contribution to Alzheimer's disease. Biochim Biophys Acta. 2010; 1801:906–916. [PubMed: 20170745]

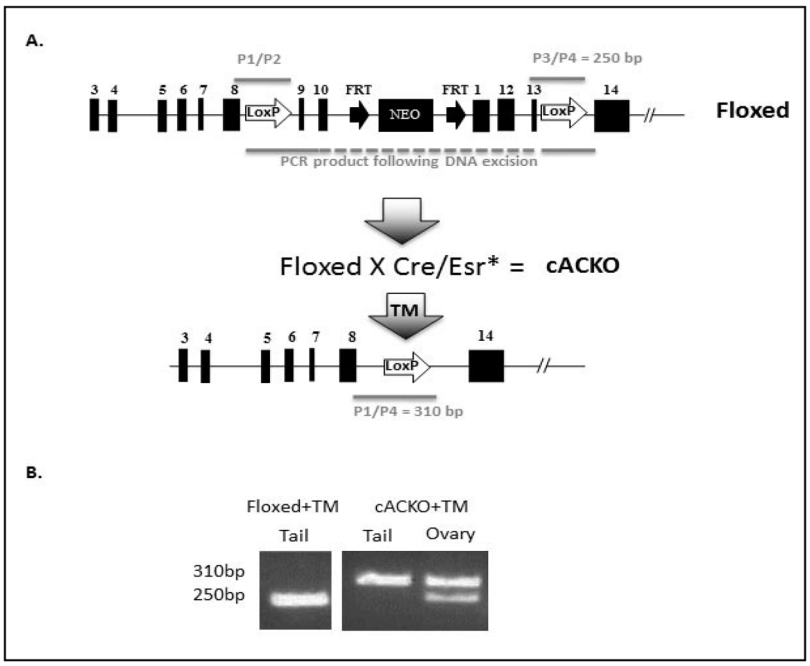

Fig. 1.

Generation of the cACKO mouse model. (A) Schematic depiction of the mouse AC gene modification, showing the Floxed allele before and after TM-induced Cre recombinase-mediated exision. The location of the primers used to detect the Floxed allele (P1/P2 and P3/P4), as well as the primers used to detect the gene rearrangement (P1/P4) also are shown. (B) Representative genotype analysis of a Floxed and cACKO mouse after TM treatment. The 250 bp band derived from within intron 13 (see Fig. 1A) is diagnostic of the Floxed allele, while the 310 bp band is derived from the gene rearrangement. Note that in the TM-treated Floxed mouse, no gene rearrangement occurred in the tail (due to the lack of Cre recombinase expression), while in the tail of the TM-treated cACKO mouse there was 100% conversion. In contrast, in the ovary of this same TM-treated cACKO mouse the gene rearrangement was partial.

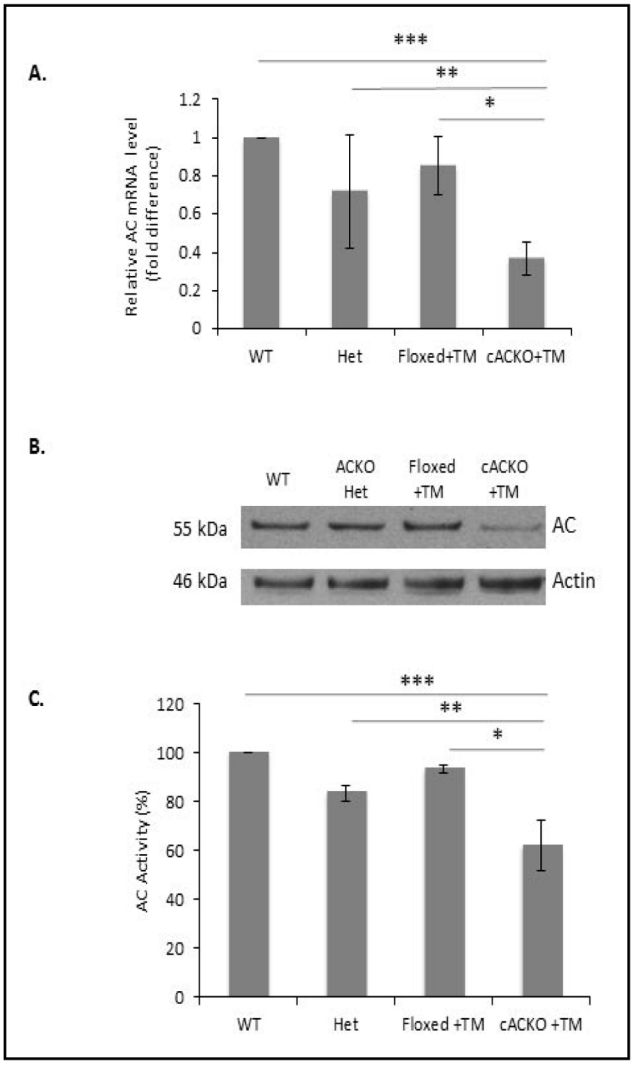

Fig. 2.

Decreased AC expression in the ovaries of TM-treated cACKO mice. (A) qPCR was used to quantify the levels of the AC mRNA in the ovaries of wild-type (WT), heterozygous complete AC knockout (Het), Floxed mice treated with TM (Floxed+TM), and cACKO mice treated with TM (cACKO+TM). The AC mRNA levels were normalized to SRP18 rRNA as an internal control. Bar heights represent the mean values (fold difference comparing AC to SRP18 expression) from 3 independent experiments. The results showed that the AC mRNA levels were significantly decreased compared to any of the three control groups (t test, P=4.02E-6 for WT mice***, 2E-2 for Het mice**, and 1.7E-4 for Floxed+TM mice*). (B) Western blot analysis showing the levels of AC precursor protein relative to beta actin. Only the cACKO mice treated with TM exhibited a reduction in AC protein levels. Blot is representative of three independent experiments. (C) Significantly decreased AC activity was observed in the ovaries of TM-treated ACKO mice, but not TM-treated Floxed mice (*=t test, P=3E-4 TM-treated cACKO compared to compared to WT mice***, 1E-3 compared to Het mice**, and 6E-3 compared to Floxed mice*).

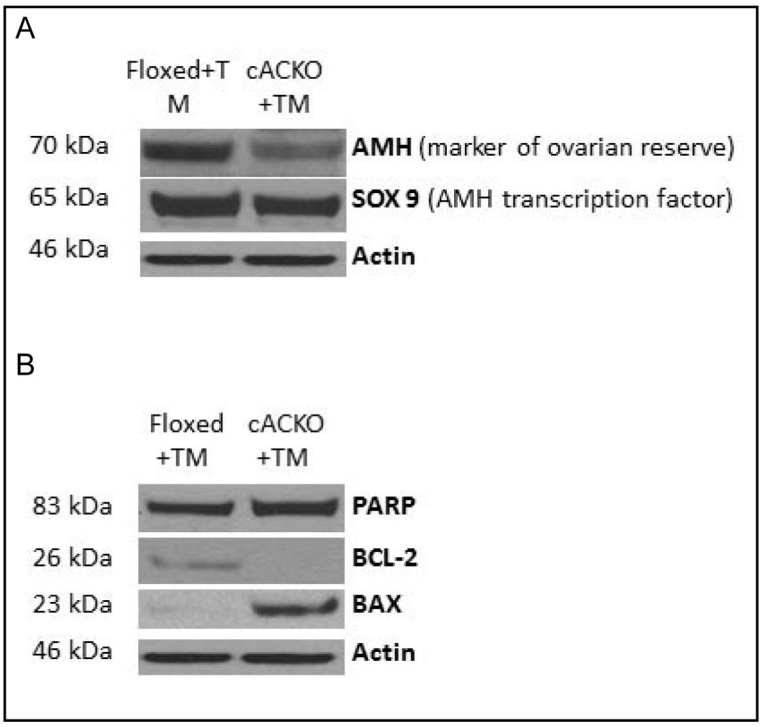

Fig. 3.

Decreased fertility in TM-treated cACKO can be explained by decreased ovarian reserve and apoptosis in the ovary. (A) Western blot analysis revealed a decreased in AMH levels, a marker of ovarian reserve, and its transcription factor Sox-9 in the ovaries of TM-treated cACKO, but not TM-treated Floxed mice. Beta actin was used as a loading control. (B) An increase in the apoptosis markers, PARP and Bax, and a decrease in the anti-apoptosis marker, Bcl-2, also was observed in the ovaries of TM-treated cACKO, but not Floxed mice. Blots are representative of three independent experiments.

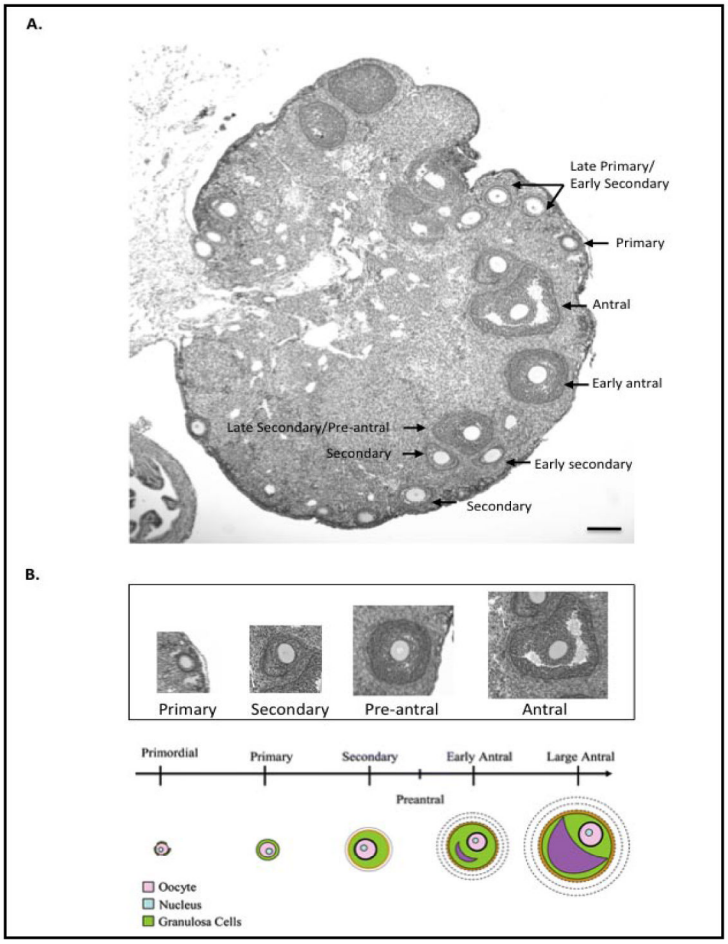

Fig. 4.

Depiction of follicles in the mouse ovary. (A) A representative H & E stained ovary section from a 3-month-old wild-type female mouse. Scale bar = 50 microns. (B) A higher magnification depicting a representative follicle at each stage. A schematic presentation of the different stage follicles also is provided below (adapted from http://amh-tes,com/).

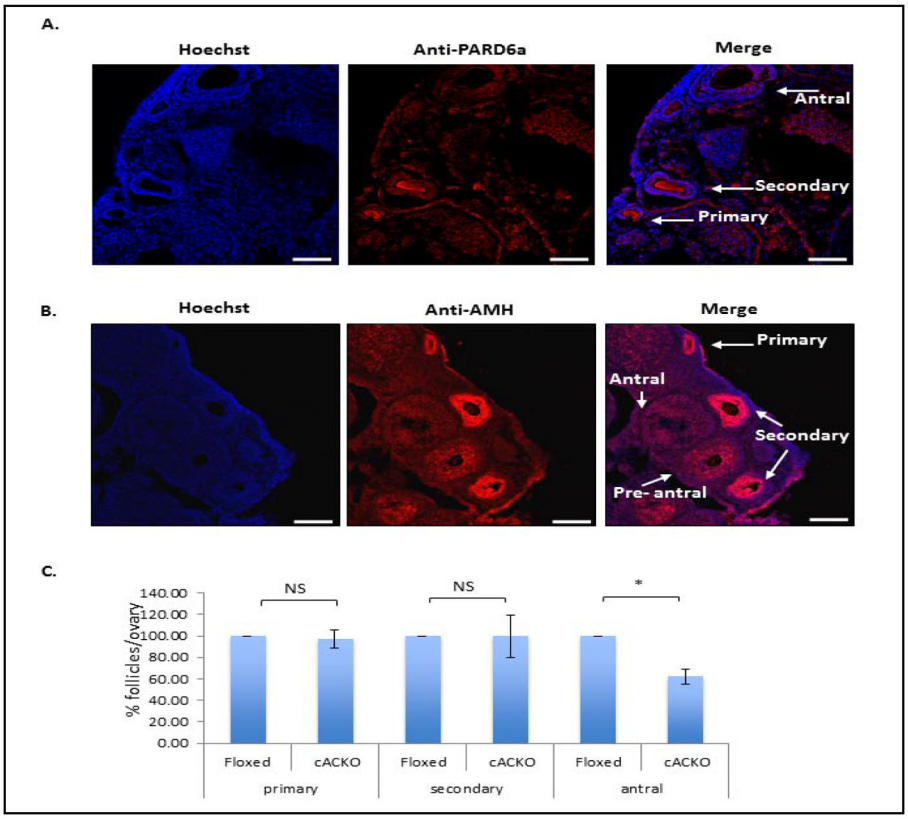

Fig. 5.

Number of follicles at different stages of maturation in TM-treated Floxed and cACKO mice. (A,B) Sample images showing immunostaining using anti-PARD6a and anti-AMH antibodies. PARD6a antibodies assist in the visualization of early stage (primary, early secondary) follicles, while AMH antibodies label secondary and early antral stages. Some labeling of primary follicles also was observed. Localization of the primary antibodies was visualized using a fluorescent second antibody (Cy-3/2) and laser scanning confocal microscopy. Scale bar = 50 microns. (C) Combined number of follicles per ovary in TM-treated cACKO and Floxed mice, assessed as described in the Materials and Methods by a combination of light microscopy and PARD6a and AMH immunostaining. Sterology was performed using the Stero Investigator software. A significant (*t-test, P=0.0002) difference was observed among the antral follicles. NS= non-significant.

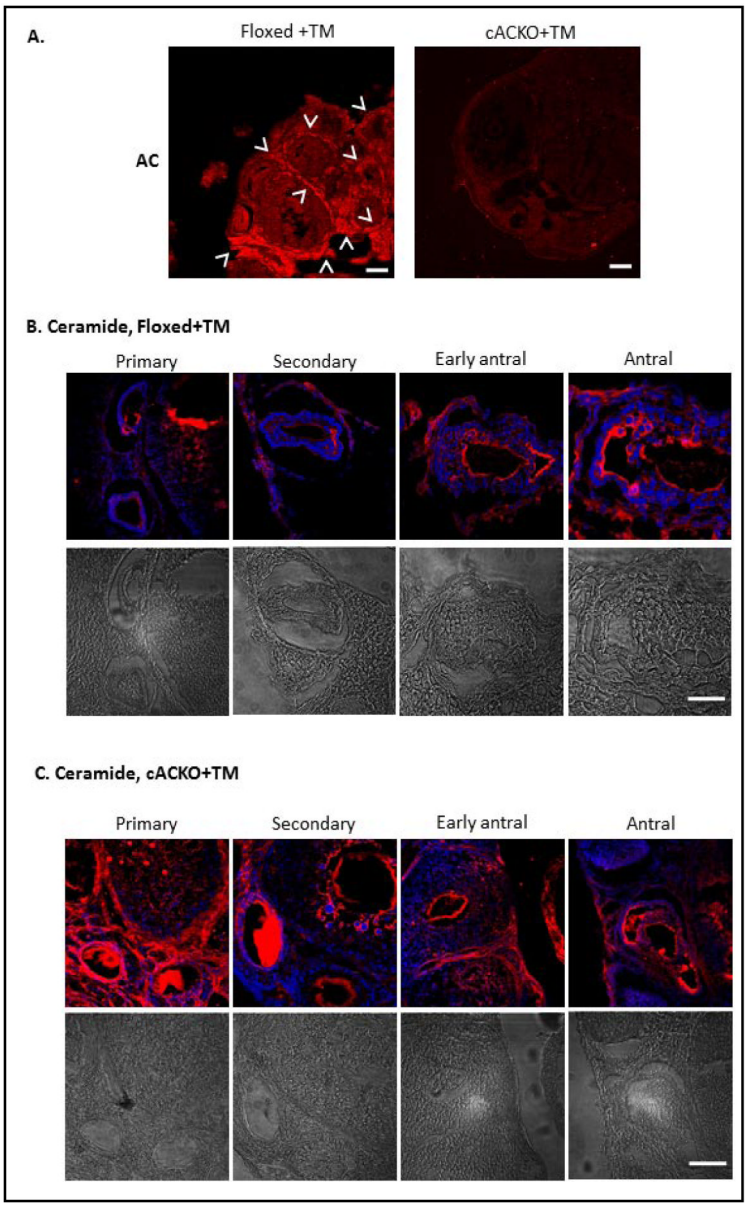

Fig. 6.

Reduced AC and elevated ceramide in the ovaries of TM-treated cACKO compared to Floxed mice. (A) High AC expression was observed by immunostaining in the ovaries of TM-treated Floxed mice. Arrowheads indicate the theca cells, where AC expression was most prominent. In contrast, AC expression levels were markedly reduced in the ovaries of TM-treated cACKO mice. AC was visualized using a fluorescent second antibody Cy-3 and laser-scanning confocal microscopy. Scale bars indicate 50 microns. Images are representative of more than three independent immunostaining experiments. (B,C) Confocal analysis of ceramide in TM-treated Floxed and cACKO mice. Ceramide was highly elevated in the primary and secondary follicles of TM-treated cACKO (C) compared to Floxed animals (B). Scale bars = 10 microns. Images are representative of three independent immuno-staining experiments. Representative follicles of each stage are shown. Light microscopic images are provided below the immunostained images.

Table 1

Decreased fertility in TM-treated cACKO mice

	cACKO+TM	Floxed+TM
Number Of Mating Pairs	13	12
Number Of Pregnancies	4	10
Number of Births	1	10
& Fertility/Fecundity	7	83